J. Biochem. **133**, 371–376 (2003)
DOI: 10.1093/jb/mvg049

Characterization of Folding Pathways of the Type-1 and Type-2 Periplasmic Binding Proteins MglB and ArgT

Kenji Kashiwagi[1,2], Kiyotaka Shiba[*,2], Kaoru Fukami-Kobayashi[4], Tetsuo Noda[3,5], Ken Nishikawa[4] and Hiroshi Noguchi[1]

[1]School of Pharmaceutical Sciences, University of Shizuoka, 52-1 Yada, Shizuoka 422-8526; [2]Department of Protein Engineering, and [3]Department of Cell Biology, Cancer Institute, Japanese Foundation for Cancer Research, 1-37-1 Kami-Ikebukuro, Toshima-ku, Tokyo 170-8455; [4]National Institute of Genetics, 1111 Yada, Mishima, Shizuoka 411-8540; [5]Department of Molecular Genetics, University of Tohoku School of Medicine, 2-1 Seiryo-cho, Aoba-ku, Sendai 980-8575

Received January 8, 2003; accepted January 9, 2003

The family of periplasmic binding proteins (PBPs) is believed to have arisen from a common ancestor and to have differentiated into two types. At first approximation, both types of PBPs have the same fold pattern, reflecting their common origin. However, the connection between the main chains of a type 2 PBP is more complicated than a type 1 PBP's. We have been interested in the possibility that such structural changes affect the folding of PBPs. In this study, we have characterized the folding pathways of MglB (a type 1 PBP) and ArgT (a type 2 PBP) by using urea gradient gel electrophoresis, fast protein size–exclusion liquid chromatography and hydrophobic dye ANS binding assay. We found a distinct difference in folding between these two proteins. The folding of MglB followed a simple two-state transition model, whereas the folding of ArgT was more complicated.

Key words: evolution of protein folding, periplasmic binding protein, protein folding, urea gradient gel electrophoresis.

Abbreviations: ANS, 8-anilino-1-naphthalenesulfonic acid; Carb, carbenicillin; PBP, periplasmic binding protein; UGGE, urea gradient gel electrophoresis.

In general, the tertiary structures of proteins are more conserved than the primary structures. For example, human hemoglobin α-chain and insect (*Chironomus thummi thummi*) larval hemoglobin share only 12.4% sequence identity, but their tertiary structures are superimposable to within 2.08 Å r.m.s (*1*). This apparent conservation of tertiary structure may be explained by the neutrality of amino acid substitutions with respect to the folding integrity (*2*). Still, protein folding does change through evolution. One mechanism for the change of folding pattern is 3D domain swapping, whereby protein folding evolves through sequence changes, insertions and deletions (*3*). Secondary structures have been shown to alter by the substitution of amino acid residues (*4*).

We have been interested in the evolution of the family of periplasmic binding proteins (PBPs), which play a pivotal role in the transport of numerous low molecular weight compounds from the extracellular milieu into the cytoplasm of bacterial cells. Forty-nine PBPs are predicted to be encoded in the *E. coli* genome (*5*), each of which recognizes specific ligands in the periplasmic space and passes them to its cognate ATP-Binding Cassette (ABC) transporter protein in the inner membrane (*6*).

PBPs consist of two symmetrical domains, each of which possesses a CheY-like fold (*7*, *8*) comprised of five α/β units (Fig. 1a), and it has been proposed that the protein ancestor of the PBP family evolved through duplication and subsequent fusion of a parental CheY-like domain (*9*, *10*) (Fig. 1b). This hypothesis is supported by the observation that the N-terminal domain of Spo0A forms either a monomeric CheY fold or a dimeric strand-swapping fold depending on the crystallization conditions (*10*), though the latter appears to be an artificial state occurring at low pH (*11*). Moreover, Fukami-Kobayashi *et al*. (*9*) showed that PBP proteins can be classified into two types based on the topologies of their folding, and that this classification is consistent with the evolutionary history inferred from phylogenic analysis of ABC proteins, which along with PBPs make up the operon. From these and other observations, they concluded that type-2 PBPs evolved from type-1 PBPs by exchanging segments of β-strand between two symmetrical domains (Fig. 1, c and d).

We are interested in the possibility that such structural changes affect the folding of PBPs. In this study, therefore, we used urea gradient gel electrophoresis (UGGE) , fast protein size-exclusion liquid chromatography and hydrophobic dye (ANS, 8-anilino-1-naphthalenesulfonic acid) binding assay to characterize the folding of MglB, a type-1 PBP involved in the transport of glucose and galactose (*12*), and ArgT, a type-2 PBP involved in the transport of lysine, arginine and ornithine (*13*).

[*]To whom correspondence should be addressed. Tel: +81-3-3918-0111, Fax: +81-3-5394-3903, E-mail: kshiba@jfcr.or.jp

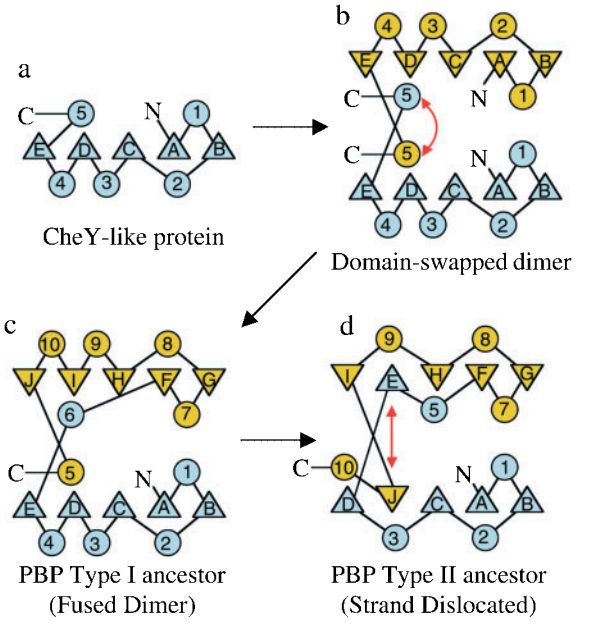

Fig. 1. **Topological diagram showing the evolution of PBP folding.** The secondary structural elements are drawn as triangles (β-strands) and circles (α-helixes). (a) CheY-like protein monomer. (b) Ancestral domain-swapped dimer. (c) PBP Type1 ancestor. (d) PBP Type2 ancestor (strand dislocated). The respective domains are colored light blue and yellow; red arrows show the secondary structural elements swapped between dimers or domains.

MATERIALS AND METHODS

Construction of Expression Vectors—Chromosomal DNA fragments coding for MglB (*12*) and ArgT (*14*) were amplified by PCR from Kohara λ clones 365 and 406, which carry the *E. coli mglB* and *argT* loci (*15*). The following oligonucleotide PCR primers were designed so that (i) the regions that encode the signal sequences of these proteins were deleted in the amplified DNAs; (ii) the *Nde*I sites were introduced at the first codons of the amplified genes; and (iii) *Xho*I sites were introduced at 3′ non-coding regions of the genes for expression of a C-terminal His-tag fusion protein: for *mglB*, KY-1259 (5′-GCA CAA CAT ATG GAT ACT CGC ATT GGT-3′) and KY-1238 (5′-G CTC GAG ACT AGT TTT CTT GCT GAA TTC AGC CAG GT-3′); for *argT*, KY-1261 (5′-TCC AGC CAT ATG GCG CTA CCG GAG ACG-3′) and KY-1252 (5′-G CTC GAG ACT AGT GTC ACC GTA GAC ATT AAA GTC G-3′). Reactions were run in a GeneAmp 9600 temperature cycler (Perkin Elmer, Norwalk); the cycling protocol consisted of 30 cycles of 30 s at 94°C, 30 s at 60°C and 60 s at 72°C. The amplified DNA fragments were purified using a Gene Clean II Kit (Qbiogene, Carlsbad), digested with *Nde*I and *Xho*I restriction endonucleases, and separated by 1.0% agarose gel electrophoresis. DNA fragments of expected size were recovered from the gel and purified using a Gene Clean II Kit, then ligated into the *Nde*I–*Xho*I sites of pET20b(+) expression vector (Novagen, Madison), which contains a T7 promoter (*16*). DNA sequencing confirmed that no unexpected mutations were incorporated into the clones during the amplifications, and the resultant expression plasmids, pKK031 and pKK030, respectively produced mature forms of MglB and ArgT under the control of the T7 promoter.

Protein Expression and Purification—E. coli BL21 (DE3)pLysS cells (*17*) harboring a given expression vector were cultured for 16 h at 37°C in 5 ml of Luria-Bertani (LB) medium (*18*) containing 50 μg/ml carbenicillin (Carb). The cells were then harvested by centrifugation, resuspended in the same amount of LB medium, and inoculated into 500 mLl of LB (Carb$^+$) medium. The cells were incubated at 37°C with vigorous shaking until the OD_{660} reached 0.4, then protein expression was induced by adding IPTG (isopropyl-β-D-thiogalactoside) to a final concentration of 0.1 mM. The cells were incubated for an additional 2 h, then harvested by centrifugation at 3,000 ×*g* for 15 m and stored at –80°C.

MglB and ArgT proteins were purified by gently stirring frozen bacterial cells on ice for 1 h in 5 ml of 10 mM Tris HCl (pH 8.0) containing 350 units of DNaseI (Takara Bio, Shiga) and 50 μg of lysozyme (Sigma Chemical, St. Louis). Insoluble proteins were removed from the resultant lysate by centrifugation at 20,000 ×*g* for 15 min. Soluble proteins were further purified using Ni-NTA Agarose (QIAGEN, Hilden) under non-denaturing conditions according to a manufacturer's instructions. Protein bound to the column was eluted with 500 mM imidazole, and the eluate was dialyzed against 10 mM sodium phosphate (pH 7.5), concentrated to 3–6 mg/ml using a CENTRIPREP 10 (Amicon, Beverly), and stored at –20°C.

Transverse Urea Gradient Gel Electrophoresis (UGGE)—Transverse liner urea gradient polyacrylamide gels were prepared essentially as described by Creighton (*19*), with slight modifications. Briefly, slab gels (74 mm × 100 mm × 1 mm) comprised of a vertical linear gradient of 0–8 M urea and a compensating 11–7% (w/v) gradient of acrylamide were prepared using a Daiichi gradient maker (Daiichi Pure Chemicals, Tokyo). After polymerization, the gels were turned 90° and fitted to the electrophoresis chamber (Daiichi Pure Chemicals). In this configuration, the gels have a transverse urea gradient so that when a uniform sample is applied over the top of the gel, different portions of the protein band migrate in different concentrations of urea.

Both native and denatured samples were subjected to transverse UGGE. For native samples, the proteins were diluted in electrophoresis buffer (0.192 M Tris glycine, pH 8.8) containing 10% glycerol and 0.02% bromophenol blue; for unfolded samples, proteins were diluted in the same buffer containing 8 M urea. Electrophoreses were carried out at 20 mA for 2 h at 4°C. After electrophoreses, the gels were stained with Phast Gel Blue R Coomassie R 350 dye (Pharmacia Biotech, Uppsala).

Size-Exclusion Chromatography—Size exclusion chromatography was carried out using an FPLC system (Pharmacia Biotech) equipped with a Superose12 10/30 column, a UV-MII detector and a zinc lamp. The column was equilibrated with 50 mM sodium phosphate (pH 7.5) containing 150 mM NaCl and the indicated concentration of urea. Chromatograms were recorded at 4°C and a flow rate of 0.3 ml/min by measuring the absorbance at 214 nm. Samples were prepared in the same buffer at low concentration (approximately 100 μg/ml) to avoid the influence of protein association, and incubated at ambient temperature for 30 min prior to application. Stokes

radii were determined by calibrating the column with thyroglobulin, catalase, albumin, ovalbumin, chymotrypsinogen, and ribonuclease A (Pharmacia Biotech).

ANS Binding Assay—Fluorescence of 8-anilino-1-naphthalenesulfonic acid (ANS) was recorded with an FP-6500 fluorescence spectrophotometer (Japan Spectroscopic, Tokyo) by using a 3-mm path length microcuvette. Samples that contained 3.3 μM protein, 50 μM ANS, 50 mM sodium phosphate pH 7.5, 150 mM sodium chloride, and various concentrations of urea were equilibrated for 16 h at room temperature before measurement. Emission at 483 nm was recorded with excitation at 375 nm (band width = 5 nm).

RESULTS

Urea Gradient Gel Electrophoresis of MglB and ArgT—To determine whether MglB and ArgT follow distinct folding pathways, we first analyzed the kinetics of their folding using UGGE (*19*). The hydrodynamic volumes of proteins reflect the state of their folding; consequently, tightly folded proteins migrate relatively rapidly in a polyacrylamide gel, whereas unfolded (denatured) proteins migrate more slowly (*20*). UGGE enables one to obtain a continuous measure of hydrodynamic volume as a function of urea concentration—folded proteins predominate at low urea concentrations, with the proportion of unfolded protein increasing as the concentration of urea increases—which provides insight into the kinetics of the transition between the folded and unfolded states.

Figure 2a shows the result obtained when the native (folded) form of MglB was analyzed by UGGE. Note that there were two clear bands. The one migrating rapidly in the low urea area represents the compact, native form of MglB, and the other more slowly migrating band in the high urea area represents the denatured (unfolded) form of MglB. These two bands are connected by a smeared band, resulting in a sigmoidal transition between the folded and unfolded states of the protein. A similar sigmoidal pattern with a smeared connecting curve was also obtained when urea-unfolded MglB was applied to the gel (Fig. 2b). These smeared bands indicate that the rates of unfolding and refolding of MglB were apparently slow, comparable to the period of electrophoresis (2 h in these experiments). The slow rates of folding and refolding were confirmed by the finding that the transition midpoints of the sigmoidal curves were different for native and denatured MglB (approximately 3.0 and 2.0 M urea, respectively). If the rates of unfolding and refolding had been rapid enough, smooth sigmoidal curves with identical transition midpoints would have been obtained (*19*).

Interestingly, qualitatively different profiles were obtained from UGGE analyses of ArgT. When the native (folded) form of ArgT was run, a sigmoidal curve similar to that generated with MglB was obtained (Fig. 2c). On the other hand, when the unfolded form of ArgT was run, two bands appeared in the low urea area (Fig. 2d), indicating the presence of two populations of unfolded proteins (*19*). Moreover, one population of unfolded ArgT apparently refolds so slowly that it remained completely unfolded during the period of electrophoresis, resulting in a straight line across the gel.

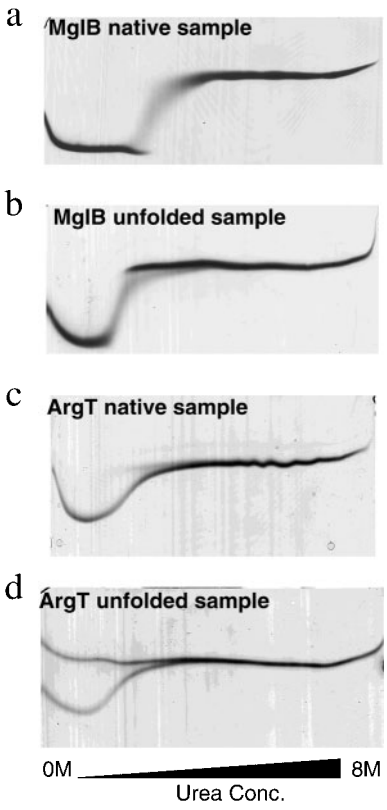

Fig. 2. **Transverse urea gradient gel electrophoresis of MglB and ArgT.** (a and c) Migration of native MglB and ArgT, respectively. (b and d) Migration of unfolded (in 8 M urea) MglB and ArgT, respectively.

Size-Exclusion Chromatography of MglB and ArgT—The observations obtained with UGGE suggest that whereas the unfolding and refolding of MglB follows a simple, two-state transition model, the folding of ArgT follows a more complicated pathway that involves unfolded proteins existing in two states. We confirmed these findings using fast protein size-exclusion liquid chromatography (*21*). We carried out gel filtration chromatography in which MglB or ArgT was applied to the column in various concentrations of urea (Fig. 3). When MglB was run through the column without urea or in the presence of 1.0 M or 1.5 M urea, the protein was eluted at 12.8–13.4 ml, which corresponds to a Stokes radius of 31.8 to 39.7 Å. In the presence of a comparatively high concentration of urea (3, 4, or 8 M), MglB behaved as a larger protein with a Stokes radius of 61.0 to 71.8 Å, indicating that it was unfolded. In the presence of 2.0 or 2.5 M urea, the sample was eluted with two peaks, which are thought to that should correspond to the unfolded and folded states of the protein (Fig. 3a). In addition, this bimodal distribution of retention times indicates that the transition between the folded and unfolded conformations of MglB is slow relative to the period of chromatography (50 min in these experiments) (*22*).

When ArgT was run in the presence of high (8 M) and low (0, 1.0, 2.0, and 2.5 M) concentrations of urea, the protein was eluted as one peak corresponding to the unfolded and folded states, respectively. In the presence

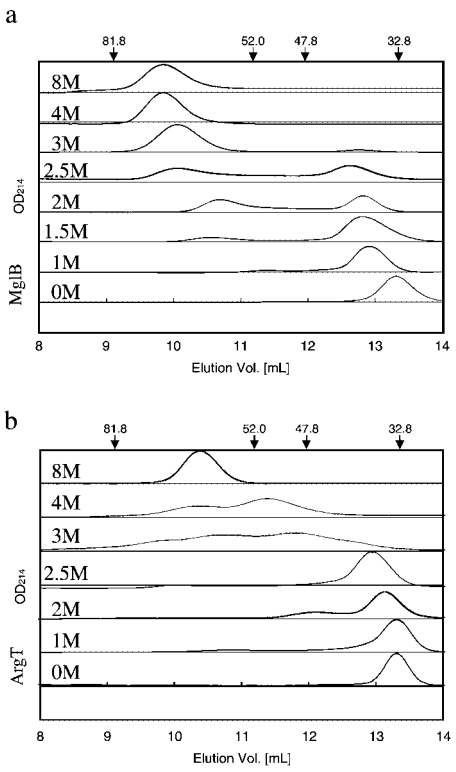

Fig. 3. **Size-exclusion chromatography elution profiles showing the unfolding of MglB (a) and ArgT (b).** Two separate peaks were observed at 2–3 M urea with MglB or 3–4 M urea with ArgT. Stokes radii of unfolded standards in 8 M urea are shown at the top of each chromatogram.

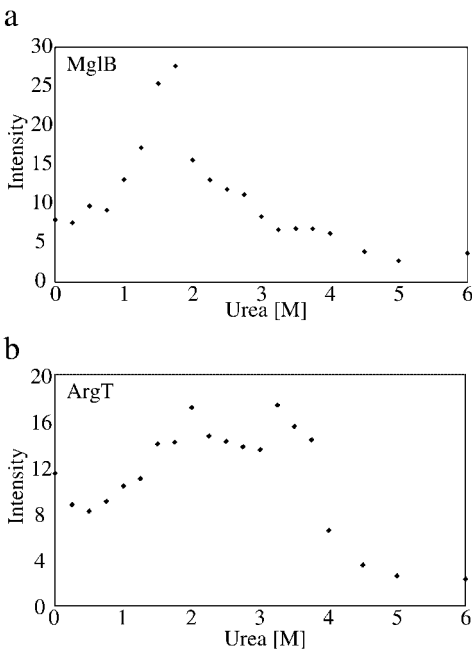

Fig. 4. **ANS binding assay for MglB (a) and ArgT (b).** Intensities of ANS fluorescence are plotted at various concentrations of urea. The indicated values are corrected for background fluorescence (without protein).

of 3 or 4 M urea, by contrast, ArgT was eluted in broad volumes with two peaks. The elution volume of one peak corresponded to protein that was fully unfolded, which may represent the population that remained unfolded in the low concentration of urea in the UGGE experiment (Fig. 2d). The second peak was located between the folded and unfolded protein, which is a typical elution profile for proteins that fold and unfold through a molten globule state (*21*).

ANS Binding of MglB and ArgT—The hydrophobic fluorescent dye ANS has been shown to bind to hydrophobic patch of the folding intermediate of proteins, and has been used to probe folding intermediates of proteins (*23*). We have assessed the ANS binding to MglB and ArgT by monitoring fluorescence intensity of ANS in the presence of various concentrations of urea. The binding profile of MglB showed the maximum fluorescence intensity at 2 M urea (Fig. 4a), which correlates with the observation in size-exclusion chromatography experiment (Fig. 3a), that is, the peaks of both folded and unfold states of the protein appeared at the same time in the presence of 1.5–3 M urea. The ANS binding profile of MglB suggested the presence of a hydrophobic folding intermediate (*24*). By contrast, binding of ANS to ArgT showed two maxima of fluorescent intensity around 2 and 3 M (Fig. 4b), suggesting the presence of two folding intermediates. This complexes profile of ANS binding showed good agreement with the existence of more than two peaks in size-exclusion chromatography under 3–4 M urea concentration (Fig. 3b), and the second band on the upper side of the gel observed in UGGE in the range of 2–3 M urea concentration (Fig 2c).

DISCUSSION

3D Domain Swapping and the Evolution of Protein Folds—The PBP family of proteins is responsible for transport of numerous low molecular weight compounds from the extracellular milieu into the cytoplasm of bacterial cells. Their ligands are, in most cases, bound in a cleft formed by two CheY-like domains. Upon ligand binding, the structures of individual domains do not change, but their configuration does (*25*). In fact, the movement of CheY-like domains upon ligand binding has been utilized in the development of biosensors (*26–28*).

It has been proposed that the first PBP emerged through tandem duplication and subsequent fusion of a parental gene—one that might have coded for a CheY-like fold (*7*, *10*). In addition, the last α-helical element was exchanged between the two CheY-like folds, either before or after the gene fusion event (Fig. 1b). Such domain swapping between monomeric proteins has been experimentally achieved by deleting amino acids (*29*, *30*), by alternating the identities of several amino acid residues (*31*, *32*), or by simply making the pH of protein solution acidic (*10*). Given the relative ease with which evolution of a new fold through exchange of strands between two similar or identical genetic units can proceed, it might be expected that domain swapping events have occurred often during the course of protein evolution and may thus represent a key mechanism by which new folds evolve (*3*, *33*).

The swapped PBP segments correspond to the hinge region that connects the two CheY-like domains and is composed of flexible loops that enable the aforementioned change in domain configuration (*8*, *34*). Thus, ligand recognition through configurational changes is premised on the flexibility of the hinge region that connects two CheY-like domains, and this flexibility might be an intrinsic propensity of peptides formed through 3D strand swapping. Intriguingly, however, the metal-binding PBP-like protein TroA contains a long stiff helix in the hinge region instead of a flexible loop so that, in contrast to canonical PBPs, the configuration of the two domains of TroA does not change upon the binding of its ligand, Zn^{2+} (*35*, *36*).

Type-1 PBPs exchange one α-helix between the two domains, whereas type-2 PBPs consecutively exchange one α-helix and then one β-strand. Fukami-Kobayashi *et al*. proposed that type-2 PBPs evolved from type-1 PBPs by exchanging an additional secondary element between the two domains (*9*). It is not known for certain whether this structural evolution is related to the protein's specific functional evolution. It is noteworthy, however, that only small ligands such as amino acids and monosaccharides are recognized by type-1 PBPs, but larger ligands such as oligopeptides (*37*), maltodextrin (*25*) and alginic acid (*38*) are recognized by type-2 PBPs. It is, therefore, possible that evolution from type-1 to type-2 was required to evolve PBPs that transport larger molecules.

Distinct Folding Kinetics of MglB and ArgT—That fact type-2 PBPs exchanged two secondary elements gives them a more convoluted topology than type-1 PBPs (Fig. 1). Whereas MglB exhibits folding kinetics typical of a simple transition between folded and unfolded states, the folding kinetics of ArgT are more complex and suggest the co-existence of an unfolded state and a molten globule state (Figs. 2 and 3). ANS binding assay has also suggested the distinct folding pathways in these two proteins (Fig. 4). Similarly, previous analysis of MBP, another type 2 PBP, showed it to assume two intermediate states during the folding reaction (*39*).

We are grateful to Dr. Y. Isogai for useful discussions. This work was supported by a Grant-in-Aid for Scientific Research from the Ministry of Education, Culture, Science, Sports and Technology of Japan.

REFERENCES

1. Aronson, H.E., Royer, W.E., Jr., and Hendrickson, W.A. (1994) Quantification of tertiary structural conservation despite primary sequence drift in the globin fold. *Protein Sci.* **3**, 1706–1711
2. Chothia, C. and Lesk, A.M. (1986) The relation between the divergence of sequence and structure in proteins. *EMBO J.* **5**, 823–826
3. Bennett, M.J., Schlunegger, M.P., and Eisenberg, D. (1995) 3D domain swapping: a mechanism for oligomer assembly. *Protein Sci.* **4**, 2455–2468
4. Cordes, M.H., Burton, R.E., Walsh, N.P., McKnight, C.J., and Sauer, R.T. (2000) An evolutionary bridge to a new protein fold. *Nat. Struct. Biol.* **7**, 1129–1132
5. Paulsen, I.T., Sliwinski, M.K., and Saier, M.H., Jr. (1998) Microbial genome analyses: global comparisons of transport capabilities based on phylogenies, bioenergetics and substrate specificities. *J. Mol. Biol.* **277**, 573–592
6. Boos, W. and Lucht, J.M. (1999). Periplasmic binding protein-dependent ABC transporters in *Escherichia coli* and *Salmonella typhimurium* (Neidhardt, F.C., ed.) Vol. **1**, pp. 1175–1209, American Society for Microbiology, Washington, DC
7. Quiocho, F.A. and Ledvina, P.S. (1996) Atomic structure and specificity of bacterial periplasmic receptors for active transport and chemotaxis: variation of common themes. *Mol. Microbiol.* **20**, 17–25
8. Murzin, A.G., Brenner, S.E., Hubbard, T., and Chothia, C. (1995) SCOP: a structural classification of proteins database for the investigation of sequences and structures. *J. Mol. Biol.* **247**, 536–540
9. Fukami-Kobayashi, K., Tateno, Y., and Nishikawa, K. (1999) Domain dislocation: a change of core structure in periplasmic binding proteins in their evolutionary history. *J. Mol. Biol.* **286**, 279–290
10. Lewis, R.J., Muchova, K., Brannigan, J.A., Barak, I., Leonard, G., and Wilkinson, A.J. (2000) Domain swapping in the sporulation response regulator Spo0A. *J. Mol. Biol.* **297**, 757–770
11. Lewis, R.J., Scott, D.J., Brannigan, J.A., Ladds, J.C., Cervin, M.A., Spiegelman, G.B., Hoggett, J.G., Barak, I., and Wilkinson, A.J. (2002) Dimer formation and transcription activation in the sporulation response regulator Spo0A. *J. Mol. Biol.* **316**, 235–245
12. Boos, W., Lengeler, J., Hermann, K.O., and Unsold, H.J. (1971) The regulation of the beta-methylgalactoside transport system and of the galactose binding protein of *Escherichia coli* K12. *Eur. J. Biochem.* **19**, 457–470
13. Nikaido, K. and Ames, G.F. (1992) Purification and characterization of the periplasmic lysine-, arginine-, ornithine-binding protein (LAO) from *Salmonella typhimurium*. *J. Biol. Chem.* **267**, 20706–20712
14. Nonet, M.L., Marvel, C.C., and Tolan, D.R. (1987) The *hisT-purF* region of the *Escherichia coli* K-12 chromosome. Identification of additional genes of the *hisT* and *purF* operons. *J. Biol. Chem.* **262**, 12209–12217
15. Kohara, Y., Akiyama, K., and Isono, K. (1987) The physical map of the whole *E. coli* chromosome: application of a new strategy for rapid analysis and sorting of a large genomic library. *Cell* **50**, 495–508
16. Studier, F.W., Rosenberg, A.H., Dunn, J.J., and Dubendorff, J.W. (1990) Use of T7 RNA polymerase to direct expression of cloned genes. *Methods Enzymol.* **185**, 60–89
17. Studier, F.W. (1991) Use of bacteriophage T7 lysozyme to improve an inducible T7 expression system. *J. Mol. Biol.* **219**, 37–44
18. Sambrook, J. and Russel, D.W. (2001. *Molecular Cloning: A Laboratory Manual*. 3rd ed., Cold Spring Habor Lab. Press, Plainview, NY
19. Creighton, T.E. (1986) Detection of folding intermediates using urea-gradient electrophoresis. *Methods Enzymol.* **131**, 156–172
20. Goldenberg, D.P. and Creighton, T.E. (1984) Gel electrophoresis in studies of protein conformation and folding. *Anal. Biochem.* **138**, 1–18
21. Uversky, V.N. (1993) Use of fast protein size-exclusion liquid chromatography to study the unfolding of proteins which denature through the molten globule. *Biochemistry* **32**, 13288–13298
22. Corbett, R.J. and Roche, R.S. (1984) Use of high-speed size-exclusion chromatography for the study of protein folding and stability. *Biochemistry* **23**, 1888–1894
23. Ali, V., Prakash, K., Kulkarni, S., Ahmad, A., Madhusudan, K.P., and Bhakuni V. (1999) 8-anilino-1-naphthalene sulfonic acid (ANS) induces folding of acid unfolded cytochrome c to molten globule state as a result of electrostatic interactions. *Biochemistry* **38**, 13635–13642
24. Semisotnov, G.V., Rodionova, N.A., Razgulyaev, O.I, Uversky, V.N., Gripas' A.F., and Gilmanshin R.I. (1991) Study of the "molten globule" intermediate state in protein folding by a hydrophobic fluorescent probe. *Biopolymers* **31**, 119–128

25. Sharff, A.J., Rodseth, L.E., Spurlino, J.C., and Quiocho, F.A. (1992) Crystallographic evidence of a large ligand-induced hinge-twist motion between the two domains of the maltodextrin binding protein involved in active transport and chemotaxis. *Biochemistry* **31**, 10657–10663
26. Marvin, J.S. and Hellinga, H.W. (2001) Conversion of a maltose receptor into a zinc biosensor by computational design. *Proc. Natl Acad. Sci. USA* **98**, 4955–4960
27. Benson, D.E., Conrad, D.W., de Lorimier, R.M., Trammell, S.A., and Hellinga, H.W. (2001) Design of bioelectronic interfaces by exploiting hinge-bending motions in proteins. *Science* **293**, 1641–1644
28. Fehr, M., Frommer, W.B., and Lalonde, S. (2002) Visualization of maltose uptake in living yeast cells by fluorescent nanosensors. *Proc. Natl Acad. Sci. USA* **99**, 9846–9851
29. Murray, A.J., Lewis, S.J., Barclay, A.N., and Brady, R.L. (1995) One sequence, two folds: a metastable structure of CD2. *Proc. Natl Acad. Sci. USA* **92**, 7337–7341
30. Green, S.M., Gittis, A.G., Meeker, A.K., and Lattman, E.E. (1995) One-step evolution of a dimer from a monomeric protein. *Nat. Struct. Biol.* **2**, 746–751
31. O'Neill, J.W., Kim, D.E., Johnsen, K., Baker, D., and Zhang, K.Y. (2001) Single-site mutations induce 3D domain swapping in the B1 domain of protein L from *Peptostreptococcus magnus*. *Structure (Camb)* **9**, 1017–1027
32. Kuhlman, B., O'Neill, J.W., Kim, D.E., Zhang, K.Y., and Baker, D. (2001) Conversion of monomeric protein L to an obligate dimer by computational protein design. *Proc. Natl Acad. Sci. USA* **98**, 10687–10691
33. Liu, Y. and Eisenberg, D. (2002) 3D domain swapping: As domains continue to swap. *Protein Sci.* **11**, 1285–1299
34. Oh, B.H., Pandit, J., Kang, C.H., Nikaido, K., Gokcen, S., Ames, G.F., and Kim, S.H. (1993) Three-dimensional structures of the periplasmic lysine/arginine/ornithine-binding protein with and without a ligand. *J. Biol. Chem.* **268**, 11348–11355
35. Lee, Y.H., Dorwart, M.R., Hazlett, K.R., Deka, R.K., Norgard, M.V., Radolf, J.D., and Hasemann, C.A. (2002) The crystal structure of Zn(II)-free *Treponema pallidum* TroA, a periplasmic metal-binding protein, reveals a closed conformation. *J. Bacteriol.* **184**, 2300–2304
36. Lee, Y.H., Deka, R.K., Norgard, M.V., Radolf, J.D., and Hasemann, C.A. (1999) *Treponema pallidum* TroA is a periplasmic zinc-binding protein with a helical backbone. *Nat. Struct. Biol.* **6**, 628–633
37. Tame, J.R., Murshudov, G.N., Dodson, E.J., Neil, T.K., Dodson, G.G., Higgins, C.F., and Wilkinson, A.J. (1994) The structural basis of sequence-independent peptide binding by OppA protein. *Science* **264**, 1578–1581
38. Momma, K., Mikami, B., Mishima, Y., Hashimoto, W., and Murata, K. (2002) Crystal structure of AlgQ2, a macromolecule (alginate)-binding protein of *Sphingomonas* sp. A1 at 2.0Å resolution. *J. Mol. Biol.* **316**, 1051–1059
39. Chun, S.Y., Strobel, S., Bassford, P., Jr., and Randall, L.L. (1993) Folding of maltose-binding protein. evidence for the identity of the rate-determining step *in vivo* and *in vitro*. *J. Biol. Chem.* **268**, 20855–20862